International Symposium
On Turbulence and Shear Flow
Phenomena (TSFP-8)
August 28 - 30, 2013 Poitiers, France

TURBULENCE MODIFICATION BY PARTICLES IN A HORIZONTAL CHANNEL FLOW

Godwin F.K. Tay
Department of Mechanical and Manufacturing Engineering
University of Manitoba
Winnipeg, MB, Canada R3T 5V6
umtayg@cc.umanitoba.ca

David C.S. Kuhn
Department of Mechanical and Manufacturing Engineering
University of Manitoba
Winnipeg, MB, Canada R3T 5V6
dkuhn@cc.umanitoba.ca

Mark F. Tachie
Department of Mechanical and Manufacturing Engineering
University of Manitoba
Winnipeg, MB, Canada R3T 5V6
tachiemf@cc.umanitoba.ca

ABSTRACT

This paper reports the results of experiments in a low Reynolds number turbulent channel flow laden with small glass particles. The effects of particles on the continuous phase turbulence were measured under conditions where the particle number density is decreasing due to sedimentation. Particles increased both the streamwise and wall-normal turbulent intensities in the wall region, but decreased the Reynolds shear stress both near the wall and in the outer layer. Two-point correlations were calculated and the results were used to provide insight into the impact of particles on the turbulence structure. It was shown that the decrease in the Reynolds shear stress is due to a reduction in correlation between the streamwise and wall-normal velocity fluctuations arising from differences in the mechanisms responsible for the increase in the two velocity fluctuation components.

INTRODUCTION

Turbulent flows laden with particles are frequently encountered in nature and in engineering. Examples include sand storms, sediment transport by rivers, pneumatic conveying of pharmaceuticals, and air-pollution control using devices such as cyclone separators and electrostatic precipitators. In most particle-laden flows, an important question that arises is whether or not particles modify the carrier fluid turbulence. The modification of the carrier fluid turbulence, which is also known as turbulence modulation, is of particular interest to researchers because changes in the carrier fluid turbulence can significantly impact the performance of particle-laden systems. Even though there is no universal parameter that can be used to reliably predict the turbulence modulation in generic turbulent flows, the general consensus is that particles ability to alter the fluid turbulence depends on a large mix of certain non-dimensional parameters. These parameters include the particle volume fraction (ϕ_v), particle Reynolds number (Re_p), particle relative diameter (d_p/L), where L represents a fluid characteristic length scale, particle Stokes number (St), particle-to-fluid density ratio (ρ_p/ρ_f), particle mass loading [$\phi_v(\rho_p/\rho_f)$], and the bulk flow Reynolds number.

Numerous studies have been conducted in the past that examined turbulence modulation by particles in wall-bounded turbulent shear flows. These include both experimental investigations (Maeda et al. 1980; Tsuji et al. 1984; Rashidi et al. 1990; Liljegren and Vlachos 1990; Kulick et al. 1994; Hagiwara et al. 2002; Kiga and Pan 2002) and numerical simulations (Pan and Banerjee 1996; Li et al. 2001; Rani et al. 2004). Nevertheless, the findings from these studies are not unanimous. For example, turbulence attenuation and augmentation have been observed respectively for small and large particles, with the degree of modification increasing with volume fraction (Maeda et al. 1980; Rashidi et al. 1990; Kulick et al. 1994; Pan and Banerjee 1996), whereas some studies indicated turbulence augmentation for small particles (Liljegren and Vlachos 1990; Rani et al. 2004).

The objective of the present work is to investigate a low Reynolds number particle-laden turbulent flow in a horizontal channel. The continuous phase is water. A particle image velocimetry (PIV) technique was used to conduct detailed velocity measurements of the fluid and

small glass particles in the streamwise – wall-normal plane of the channel. The novelty of the present work is that the statistical properties of the particles and fluid were measured in flow fields in which the particle concentration was declining. The concentration decline was initiated by adding particles to the flow and allowing some of the particles to settle out without replenishment. This is practically relevant, for example, in the estimation of the flow fields in pneumatic conveyors, sedimentation tanks and pollutant or aerosol monitoring systems where particles may be transported without a source to maintain a constant particle volumetric flux.

EXPERIMENTAL SETUP AND METHODOLOGY

The test section is a plane rectangular channel as shown schematically in figure 1. It was fabricated from 6 mm thick acrylic test plates, and has a length and internal width of 2500 mm and 186 mm, respectively. The internal height of the channel is 40 mm, which yields an aspect ratio, $b/(2h)$, of approximately 5:1, where b is the channel width and h is the channel half-height. As indicated in the figure, the x coordinate is aligned with the streamwise direction, while y and z coordinates are respectively aligned with the wall-normal and spanwise directions; $x = 0$ is at the inlet and $z = 0$ is at the mid-span. The origin $y = 0$ is on the lower wall of the channel.

The particulate phase is solid glass of density 2500 kg/m^3 and mean diameter 64 µm, sieved into a size range of 53 µm - 75 µm. Two particle volume fractions were considered: $\phi_v = 2.0 \times 10^{-4}$ and $\phi_v = 7.0 \times 10^{-4}$, which were estimated by weighing the particles. The particles were fed into the flow, and allowed to recirculate with the flow. The particle Reynolds number, $Re_p = d_p|U_{rel}|/\nu$, where U_{rel} is the relative velocity between the particles and the fluid, and ν is the fluid kinematic viscosity, was approximately 2.0 for both loading ratios. The corresponding Stokes number, $St = \tau_p/\tau_f$, where $\tau_p = \tau_{p,Stokes}/(1 + 0.15Re_p^{0.687})$ is the corrected particle response time, $\tau_{p,Stokes} = [(2\rho_p/\rho_f + 1)d_p^2]/(36\nu)$ is the Stokesian response time, τ_f is the viscous time scale, ν/U_τ^2, and U_τ is the friction velocity, was approximately 1.0. The relative particle diameter in wall units was approximately $d_p^+ = 2.2$.

The flow was tripped at the inlet of the channel using two 3 mm acrylic ribs, each affixed to one of the principal walls, to quicken boundary layer transition to turbulence. The measurements were made in the mid-plane at $x/h \approx 76$ downstream of the trip. The experiments were conducted both in clear water and in the presence of particles at a channel centreline velocity of approximately $U_{max} = 0.75$ m/s. The friction velocity estimated using the Clauser chart method was approximately 0.035 m/s. For the clear water flow, the turbulent intensity, u/U_{max}, measured at the channel centre line was about 0.04, which is in good agreement with values of 0.04 ± 10% compiled by Durst et al. (1998) for pipe and channel flows.

The velocities of the carrier fluid and particles were measured separately. The setup consists of a 12-bit 2048 pixels × 2048 pixels CCD camera, a double-pulsed Nd-YAG laser, and a PC. The velocity of the carrier fluid was detected by seeding the flow with 10 µm polymer

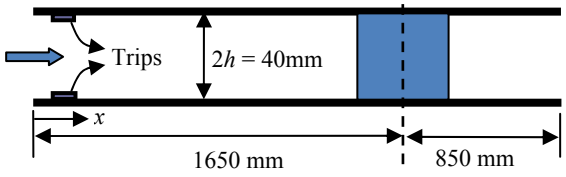

Figure 1. Schematic of the test section (not drawn to scale).

microspheres coated in Rhodamine B. Rhodamine B is a fluorescent dye that absorbs green laser light at a wavelength of 532 nm, and fluoresces with orange light at a wavelength of 590 nm. The fluorescent light from the seeding particles was separated from the Mie scattering light due to the solid phase by equipping the camera lens with a long-pass cut-off orange filter centred on the emission wavelength of the dye. The velocity of the carrier fluid was measured first. At the end of each fluid diagnostics period, the flow was vigorously agitated to bring particles that have settled back into suspension. The solid phase velocity was measured using the same camera but with the orange filter replaced by a green (band-pass) filter that captured the Mie scattering light from the solid particles. Even though the green filter exposed the camera to some Mie scattered light from the fluid tracer particles, the cross talk between the two phases was very minimal due to the size difference between the particles and tracers. Data acquisition was controlled using the DynamicStudio software developed by Dantec Dynamics. For each phase an ensemble of 5000 image pairs was acquired, which is large enough for the flow statistics to converge. The data were post-processed using the adaptive correlation option of DynamicStudio. The interrogation area (IA) size for the correlation was set to 32 pixels × 32 pixels with 50 % overlap in both x and y. The adaptive correlation algorithm used a multi-pass FFT with a one-dimensional Gaussian peak-fitting function to determine the average particle displacement within the interrogation window to sub-pixel accuracy. During the image acquisition, steps were taken to ensure that the maximum particle displacement was less than ¼ of the IA size. With an IA size of 32 pixels × 32 pixels, the maximum particle displacement in the main flow direction was 8 pixels with a dynamic range of 80. The spatial resolution and physical spacing between the velocity vectors in the y-direction were respectively 0.788 mm and 0.394 mm. In all experiments, the uncertainties in the mean velocity, turbulent intensities, and Reynolds shear stress at the 95 % confidence level were estimated as ±3 %, ±7 %, and ±10 %, respectively.

RESULTS AND DISCUSSION

All single-point statistics measured in this study were obtained by ensemble averaging over the 5000 samples and line averaging the ensemble averaged results in the streamwise direction over the field of view. The discussion is focused on turbulence modification of the carrier fluid by the particles. The influence of particles on the carrier fluid motion is first examined using single-point statistics such as the mean velocity, turbulent intensities, Reynolds shear stress and quadrant decomposition of the Reynolds shear stress. Two-point

correlations are also examined to highlight the effects of particles on the spatial structure of the flow. Because particles settled out of the flow over time by gravitational drift towards the lower wall of the channel, all statistics presented here are limited to the lower half of the channel. In order to facilitate the presentation and discussion of the results, the test conditions are designated as Φ_k, where k = 0 signifies the clear water flow, and k = 1 or 2 signifies the particle-laden flow at the lower or higher loading level.

Figure 2 shows the particle count and number density distributions of the solid phase, calculated by counting the number of particles imaged within the field of view. The plots in figures 2a and 2b show how the overall particle count per image varied in the particle-laden flows. The concentration decay is more severe for the higher volume fraction than the lower volume fraction. At the higher volume fraction, the decay is quite spectacular within the early stages of the acquisition interval. This is consistent with results from deposition studies that particles settle out of the flow more quickly as volume fraction increases. To quantify the overall decay rates in the experiments, least square exponential decay laws were fitted to the particle count data as shown in figure 2c. The curves correspond to the equations $y = y_o + be^{ax}$ for Φ_1, where $y_o = 610.15$, $b = 392.43$, $a = -9.75 \times 10^{-4}$, and $y = y_o + b_1 e^{[-(x-x1)/a1]} + b_2 e^{[-(x-x1)/a2]}$ for Φ_2, where $y_o = 723.25$, $x_1 = 20.14$, $b_1 = 7261.51$, $b_2 = 1516.02$, $a_1 = 151.20$ and $a_2 = 1412.13$. The corresponding coeffcicients of determination (R^2 values) were respectively 0.66 and 0.98. The fitted values, normalized by their corresponding initial particle counts, show that the overall decay rate is about eight times larger for Φ_2 than Φ_1. The present results are qualitatively similar to the depletion in particle count observed by Dritselis (2009) for the reference smooth wall in his study. The particle count plots in this work indicate that for a large fraction of the time the particle count is relatively constant, albeit at a lower value than the initial particle count. The results suggest the existence of two flow regimes, namely, an interval where the concentration decline is higher, which consists roughly of the first 1000 images for each loading ratio, and the interval where the concentration is relatively steady, which consists roughly of the last 4000 images. For each loading ratio, the effect of the concentration decline on the carrier fluid statistics was investigated by partitioning the data into three batches. These consist of the first 1000 images, and two sub-samples of 2000 images from the last 4000 images. The values of the mean velocity, turbulent intensities and Reynolds shear stress based on these samples were calculated. By comparing the results among the various sub-ensembles and with the overall ensemble of 5000 images, it was observed that for the lower loading ratio, the turbulent intensities and Reynolds shear stress are independent of the concentration decay. However, for the higher loading ratio, the peak value of the wall-normal turbulent intensity for the regime of steep concentration decline was about 50% larger in comparison to values calculated for the sub-ensembles in the steady regime. The streamwise turbulent intensity also increased, but only marginally. The Reynolds shear stress on the other hand

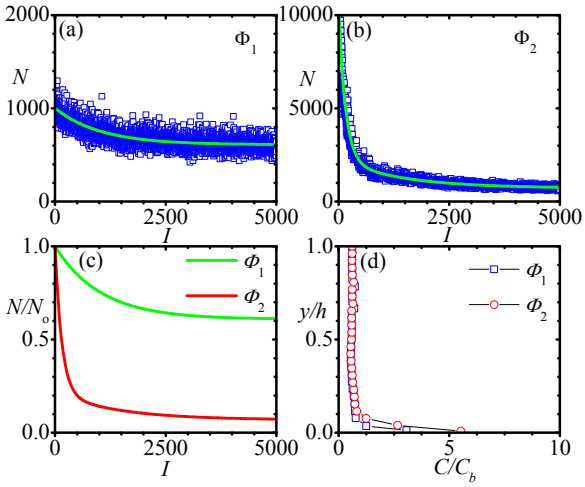

Figure 2. Particle count and number density distributions.

remained unchanged due to a reduction in the Reynolds shear stress correlation coefficient. For both loading ratios, the mean velocity shows no sensitivity to the concentration decay. Despite the differences observed for Φ_2, all statistics reported subsequently were based on the entire ensemble of 5000 images since it is the mean flow behaviour that is sought rather than focusing on a segment of the data. Figure 2d shows distributions of the mean particle number density normalized by the bulk or depth-averaged number density. The distributions show that the particle concentration is relatively constant, and have similar values for both loading ratios over most of the flow region. As observed in previous studies (Kaftori et al. 1995; Soldati 2005), the particle concentration attains a peak value very close to the wall. In general, the concentration is larger near the wall, because the low fluid velocity in this region is insufficient to entrain particles. Soldati (2005) remarked that the presence of a concentration maximum very close to the wall can be considered as a consequence of non-uniform turbulence advection mechanisms, whose intensity decrease to very low values in the near wall region.

Figure 3 shows the distributions of the mean velocity, turbulent intensities and Reynolds shear stress for the carrier fluid. The mean velocity and turbulent intensities are normalized by the maximum streamwise mean velocity U_{max}, while the Reynolds shear stress is normalized by U_{max}^2. The mean velocity U/U_{max} (Figure 3a) is slightly increased for $0.12 < y/h < 0.6$ in the presence of particles, suggesting an increase in the mean strain rate $\partial U/\partial y$ in this region. This is in agreement with mean velocity enhancements reported in previous studies (Maeda et al. 1980; Yamamoto et al. 2001; Righetti and Romano 2004). Muste et al. (2009) explained that particles tend to travel faster than the fluid in the near wall region because particles are not governed by the no slip condition at the wall. This would imply that particles moving faster than the fluid would drag the fluid along with them, which would lead to an increase in the fluid mean velocity. Particles also increased the turbulent intensities in the inner region with larger effects in the wall-normal turbulent intensity compared to the streamwise turbulent intensity. These observations are in

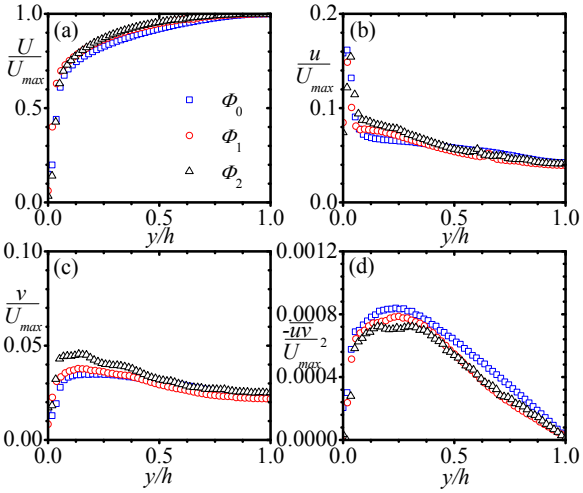

Figure 3. Distributions of the fluid mean velocity, turbulent intensities and Reynolds shear stress.

qualitative agreement with data reported in the literature. Liljegren and Vlachos (1990), for instance, found that 50 μm glass particles enhanced the carrier fluid turbulent intensity for a horizontal pipe flow by amounts that increased with volumetric loading. Regardless of the increase in the turbulent intensities, the Reynolds shear stress shows a decreasing effect in the presence of particles. These suggests that the respective increments in the streamwise and wall-normal turbulent intensities are not correlated. This may be the case when the augmentation effects in the two turbulent intensities are due to different mechanisms. The increase in the streamwise turbulent intensity for instance may be attributed to the enhanced feedback force due to the slip velocity between particles and the fluid, while that in the wall-normal turbulent intensity may be attributed to the influence of gravitational settling. Rani et al. (2004) found that the fluid streamwise turbulent intensity is increased as a result of the enhancements in the particle source term by fast moving particles. The literature also suggests that the fluid velocity fluctuation component aligned with the direction of the gravitational force tends to be strongly influenced by gravitational settling of particles. The reduced correlation between the two velocity fluctuation components is confirmed by a reduction in the single-point Reynolds shear stress correlation coefficient (not shown).

Quadrant Decomposition

Quadrant decomposition is a useful tool for examining the Reynolds shear stress producing events in turbulence. With this technique the instantaneous Reynolds shear stress $u_i v_i$ is sorted into the four quadrants of the u-v plane: Q1 (outward interactions) when both u_i and v_i are positive, Q2 (ejections) when u_i is negative and v_i is positive, Q3 (inward interactions) when both u_i and v_i are negative, and Q4 (sweeps) when u_i is positive and v_i is negative. The inward and outward interaction terms contribute only positive Reynolds shear stress, while ejections and sweeps contribute negative Reynolds shear stress. Ejections transport low-momentum fluid away from the wall to the

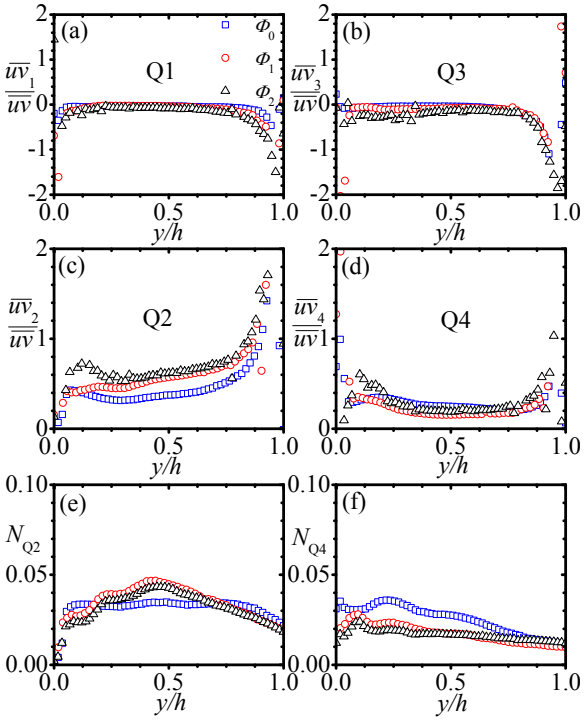

Figure 4. Quadrant decomposition of the carrier fluid Reynolds shear stress.

outer layer, while sweeps transport high-momentum fluid from the outer layer to the wall region. Following the methodology proposed by Lu and Willmarth (1973), the mean Reynolds shear stress at a given wall-normal location is decomposed into contributions from the four quadrants Q1, Q2, Q3 and Q4 excluding a hyperbolic hole of size H as

$$\langle uv\rangle_Q(x,y,H)=\frac{1}{N}\sum_{i=1}^{N}u_i(x,y)v_i(x,y)S_Q(x,y,H) \quad (1)$$

where N is the total number of instantaneous velocity vectors (= total number of PIV snapshots) at a given wall-normal location and S_Q is a detector function given by

$$S_Q(x,y,H)=\begin{cases}1, \text{ when } |u_i(x,y)v_i(x,y)|_Q \geq Hu_{rms}(x,y)v_{rms}(x,y)\\ 0, \text{ otherwise}\end{cases} \quad (2)$$

Figure 4 presents the quadrant decomposition results obtained with hyperbolic hole size H = 2. The contributions for the unladen flow are in good agreement with those presented by Krogstad et al. (2005) for a turbulent channel experiment and DNS. The quadrant decomposition shows that the outward and inward interaction terms (figures 4a and 4b) are unimportant except near the core of the channel. The results also indicate that for both the laden and unladen cases, the ejections and sweeps are the more dominant contributors to the mean Reynolds shear stress. Similar observations were reported in previous unladen and particle-laden wall-bounded turbulent flows (Krogstad et al. 2005; Kaftori et al. 1998). The plots in figures 4c and 4d suggest that particles enhanced the contributions from strong ejections (Q2) more significantly in the outer layer but the contributions from strong Q4 motions are nearly

independent of loading. Near the wall, particles increased the two contributions only at the higher loading. Results in the literature on particle effects on the quadrant contributions are varied. Kaftori et al. (1998) observed that large polystyrene particles (d_p^+ = 17.4) increased Q3 and Q4 motions more strongly, with larger effects near the wall, while Q1 and Q2 motions remained relatively unchanged. Because the large particles increased the Q4 motions more strongly than Q3, Kaftori et al. (1998) observed larger Reynolds shear stress values near the wall. Righetti and Romano (2004) found that small and medium sized glass particles (d_p^+ = 3.8 and 8.5) increased all four quadrant events near the wall and reduced them in the outer layer, leading to larger Reynolds shear stress values near the wall and smaller values in the outer layer. The distributions plotted in figures 4e and 4f indicate the proportion of ejections and sweeps residing in the second and fourth quadrants, respectively. The values of N_{Q2} can be used to provide a rough indication of the bursting frequency in the flow. Figure 4e shows that near-wall bursts are rarer in the particle-laden flows than in the clear water flow. The bursting frequency increases away from the wall for the laden flow, but falls again in the core region. The proportion of sweeps (figure 4f) is generally lower in the presence of particles compared to the clear water flow. The relative intensities of the ejections and sweeps, coupled with the trends observed in their proportions across the flow are consistent with the reduction in the Reynolds shear stress.

Two-Point Correlations

Two-point correlations are often used to investigate the spatial coherence in the velocity fluctuations due to the vortical structures. The two-point correlation function, R_{AB}, between any two arbitrary quantities $A(x, y)$ and $B(x, y)$ may be defined as

$$R_{AB}(x_{ref}+\Delta x, y_{ref}+\Delta y)=\frac{\langle A(x_{ref},y_{ref})B(x_{ref}+\Delta x,y_{ref}+\Delta y)\rangle}{\langle \sigma_A(x_{ref},y_{ref})\sigma_B(x_{ref}+\Delta x,y_{ref}+\Delta y)\rangle} \quad (3)$$

where the point (x_{ref}, y_{ref}) denotes the reference location, Δx and Δy are the spatial separations between A and B in the streamwise and wall-normal directions, respectively, and σ_A and σ_B are the root-mean-square values of A and B at (x_{ref}, y_{ref}) and (x_{ref} +Δx, y_{ref} +Δy), respectively.

The effects of particles on the two-point auto-correlation functions of the velocity fluctuations are examined in figure 5. The two-point correlations were calculated at the reference locations y/h = 0.1 and y/h = 0.4, where the location y/h = 0.1 corresponds to the wall-normal location where the largest enhancements were observed in the turbulent intensities, and y/h = 0.4 is a location in the outer layer. Both R_{uu} and R_{vv} are plotted as functions of the streamwise separation Δx. The auto-correlation function of the streamwise velocity fluctuation, R_{uu}, is more strongly affected by the particle motion than the wall-normal fluctuating velocity auto-correlation both near the wall and in the outer layer. Near the wall, R_{uu} is

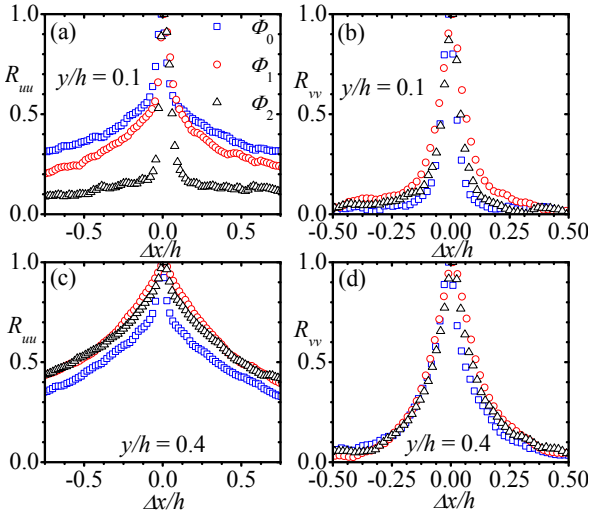

Figure 5. Streamwise distributions of the two-point auto-correlation functions.

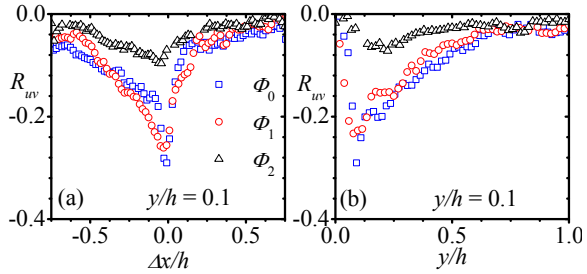

Figure 6. Streamwise and wall-normal distributions of the cross-correlation function.

attenuated by particles and the effect increases with volume fraction. In the outer layer, particles enhanced the R_{uu} correlations, but the influence of volume fraction is negligible. At both locations, the R_{vv} correlations are independent of loading. Similar observations were made for the two auto-correlation functions when plotted as functions of the wall-normal distance y/h (not shown). Figure 6 compares the two-point cross-correlation functions of the u and v fluctuations, R_{uv}, at y/h = 0.1 among the test cases. Because R_{uv} connects the Reynolds shear stress producing regions in the flow, the predominantly negative values again demonstrate the importance of ejections (Q2) and sweeps (Q4) in generating the Reynolds shear stress. At the lower loading, the deviations from the clear water distribution are within measurement uncertainty. At the higher loading however, the cross-correlation functions are dramatically reduced. These reflect the earlier observation that the Reynolds shear stress is reduced in the presence of particles due to the reduced correlation between the streamwise and wall-normal velocity fluctuations. The reduction in R_{uv} as the volume fraction is increased, produces more compact structures near the wall, which as pointed out by previous investigations (Niño and Garcia 1996; Kaftori et al. 1998) are more energetic than in the clear water flow. The relatively larger values of the

ejections and sweeps at $y/h \approx 0.1$ for Φ_2 in the quadrant decomposition plots supports this view.

SUMMARY AND CONCLUSIONS

A particle image velocimetry method was used to investigate turbulence modification by small glass particles in a horizontal channel. The experiments were conducted under conditions where the overall particle concentration in the flow is decreasing as result of gravitational settling. The results indicate enhancements in the fluid mean velocity due to the momentum imparted to the fluid by faster moving particles. Particles also enhanced the streamwise and wall-normal turbulent intensities in the inner region, but produced no significant modification in the outer layer. The presence of particles led to a reduction in the Reynolds shear stress values across the flow region because of a reduced correlation between the streamwise and wall-normal velocity fluctuations. A quadrant decomposition of the carrier fluid Reynolds shear stress shows that particles generally increase the contributions from strong ejections but leave the contributions from sweeps relatively unchanged for nearly the entire flow region. Although a modest increase did occur in the ejections and sweeps near the wall as the volume fraction increased, the proportion of these motions decreased relative to the unladen flow. Particles dampened the two-point auto-correlation functions of the velocity fluctuations near the wall but enhanced them in the outer layer. The two-point cross-correlation function was atttenuated both near the wall and in the outer layer.

REFERENCES

Best, J., Bennet, S., Bridge, J. and Leeder, M., 1997, "Turbulence Modulation and Particle Velocities over Flat Sand Beds at Low Transport Rates," *Journal of Hydraulic Engineering*, Vol. 123(12), pp. 1118-1129.

Dritselis, C.D., 2009, "LES of Particle-Laden Turbulent Channel Flow with Transverse Roughness Elements on One Wall," *Numerical Analysis and Applied Mathematics*, Vol. 2, pp. 677-680.

Durst, F., Fischer, M., Jovanovic, J., and Kikura, H., 1998, "Methods to Set Up and Investigate Low Reynolds Number, Fully Developed Turbulent Plane Channel Flows," *Journal of Fluids Engineering*, Vol. 120(3), pp. 496-503.

Hagiwara, Y., Murata, T., Tanaka, M., and Fukawa, T., 2002, "Turbulence Modification by the Clusters of Settling Particles in Turbulent Water Flow in a Horizontal Duct," *Powder Technology*, Vol. 125, pp. 158-167.

Kaftori, D., Hetsroni, G. and Banerjee, S., 1995, "Particle Behaviour in the Turbulent Boundary Layer. II. Velocity and Distribution Profiles," *Physics of Fluids*, Vol. 7(5) , pp. 1107 - 1121.

Kaftori, D., Hetsroni, G. and Banerjee, S., 1998, "Effects of Particles on Wall Turbulence," *International Journal of Multiphase Flow*, Vol. 24(3), pp. 359-386.

Kiga, K.T. and Pan, C., 2002, "Suspension and Turbulence Modification Effects of Solid Particulates on a Horizontal Turbulent Channel Flow," *Journal of Turbulence*, Vol. 3, pp. 1-21.

Krogstad, P. -Å., Andersson, H.I., Bakken, O.M. and Ashrafian, A., 2005, "An Experimental and Numerical Study of Channel Flow with Rough Walls," *Journal of Fluid Mechanics*, Vol. 530, pp. 327-352.

Krogstad, P. -Å., Antonia, R.A. and Browne, L.W.B., 1992, "Comparison between Rough-and Smooth-Wall Turbulent Boundary Layers," *Journal of Fluid Mechanics*, Vol. 245, pp. 599-617.

Kulick, J.D., Fessler, J.R. and Eaton, J.K., 1994, "Particle Response and Turbulence Modification in Fully Developed Channel Flow," *Journal of Fluid Mechanics*, Vol. 277, pp. 109-134.

Li, Y., McLaughlin, J.B., Kontomaris, K., and Portela, L., 2001, "Numerical Simulation of Particle-Laden Turbulent Channel Flow," Physics of Fluids, Vol. 13(10), pp. 2957-2967.

Liljegren, L.M., and Vlachos, N.S., 1990, "Laser Velocimetry Measurements in a Horizontal Gas-Solid Pipe Flow," *Experiments in Fluids*, Vol. 9, pp. 205-212.

Lu, S. S., and Willmarth, W. W. 1973, "Measurements of the Structure of the Reynolds Stress in a Turbulent Boundary Layer," *Journal of Fluid Mechanics*, Vol. 60, pp. 481-512.

Maeda, M., Hishida, K. and Furutani T., 1980, "Optical Measurements of Local Gas and Particle Velocity in an Upward Flowing Dilute Gas-Solids Suspension," *Proceedings of Polyphase Flow and Transport Technology*, Century 2-ETC, San Francisco, pp. 211-216.

Muste, M., Yu, K., Fujita, I., and Ettema, R., 2009, "Two-Phase Flow Insights into Open-Channel Flows with Suspended Particles of Different Densities," *Environmental Fluid Mechanics*, Vol. 9, pp. 161-186.

Niño, Y., and Garcia, M.H., 1996, "Experiments on Particle-Turbulence Interactions in the Near-Wall Region of an Open Channel Flow: Implications for Sediment Transport," *Journal of Fluid Mechanics*, Vol. 326, pp. 285-319.

Pan, Y., and Banerjee, S., 1996, "Numerical Simulation of Particle Interactions with Wall Turbulence," *Physics of Fluids*, Vol. 8 (10), pp. 2733-2755.

Rani, S.L., Winkler, C.M., and Vanka, S.P., 2004, "Numerical Simulations of Turbulence Modulation by Dense Particles in a Fully Developed Pipe Flow," *Powder Technology*, Vol. 141, pp. 80-99.

Rashidi, M., Hetsroni, G. and Banerjee, S., 1990, "Particle-Turbulence Interaction in a Boundary-Layer," *International Journal of Multiphase Flow*, Vol. 16, pp. 935-949.

Righetti, M. and Romano, G.P., 2004, "Particle-Fluid Interactions in a Plane Near-Wall Turbulent Flow," *Journal of Fluid Mechanics*, Vol. 505, pp. 93-121.

Soldati, A., 2005, "Particles Turbulence Interactions in Boundary Layers," *Zamm-Zeitschrift fur Angewandte Mathematik und Mechanik*, Vol. 85(10), pp. 683-699.

Tsuji, Y., Morikawa, Y. and Shiomi, H., 1984, "LDV Measurements of an Air-Solid Two-Phase Flow in a Vertical Pipe," *Journal of Fluid Mechanics*, Vol. 139, pp. 417-434.

Yamamoto, Y., Potthoff, M., Tanaka, T., Kajishima, T. and Tsuji, Y., 2001, "Large Eddy Simulation of Turbulent Gas-Particle Flow in a Vertical Channel: Effect of Considering Inter-Particle Collisions," *Journal of Fluid Mechanics*, Vol. 442, pp. 303-334.